Journal of Molecular Catalysis A: Chemical xxx (2015) xxx–xxx

Contents lists available at ScienceDirect

Journal of Molecular Catalysis A: Chemical

journal homepage: www.elsevier.com/locate/molcata

In situ generation of water-stable and -soluble ruthenium complexes of pyridine-based chelate-ligands and their use for the hydrodeoxygenation of biomass-related substrates in aqueous acidic medium

Thomas A. Minard[a], Christopher T. Oswin[a], Fraser D.C. Waldie[a], Jennifer K. Howell[a], Benjamin M.T. Scott[a], Domenico Di Mondo[a], Ryan J. Sullivan[a], Benjamin Stein[a], Michael Jennings[b], Marcel Schlaf[a,*]

[a] *Department of Chemistry, University of Guelph, The Guelph-Waterloo Centre for Graduate Work in Chemistry (GWC)², 50 Stone Road East, Guelph, Ontario N1G 2W1, Canada*
[b] *Department of Chemistry, Western University, 1151 Richmond Street, London, Ontario N6A 5B7, Canada*

ARTICLE INFO

Article history:
Received 27 July 2015
Accepted 29 August 2015
Available online xxx

Keywords:
Homogeneous catalysis
Ruthenium complexes
Aqueous media
Hydrogenation
Hydrodeoxygenation
Biomass conversion

ABSTRACT

The complexes [Ru(2,2′-dipicolylamine)$(OH_2)_3$]$(OTf)_2$ and [Ru(6,6′-bis(aminomethyl)-2,2′-bipyridine)$(OH_2)_2$]$(OTf)_2$ can be prepared by reaction of 2,2′-dipicolylamine or 6,6′-bis(aminomethyl)-2,2′-bipyridine with $[Ru^{III}(DMF)_6](OTf)_3$ in aqueous medium. During the reaction an *in situ* reduction from a paramagnetic Ru^{III} to a diamagnetic Ru^{II}-complexes occurs with one equivalent of DMF acting as the reducing agent for two ruthenium centres by its reaction with water and decomposition to dimethylammonium triflate and CO_2 generating an additional equivalent of HOTf in the process. The complex solutions are active as catalysts for the hydrogenation of 2,5-hexanedione and 2,5-dimethylfuran to 2,5-hexanediol and 2,5-dimethyltetrahydrofuran with both complexes realizing very high yields (>95% combined yield of the two products with the selectivity determined as a function of added acid co-catalyst). The 2,2′-dipicolylamine complex is stable to 150 °C, while the 6,6′-bis(aminomethyl)-2,2′-bipyridine complex is stable to 200 °C allowing the *in situ* hydrolysis of 2,5-dimethylfuran to the 2,5-hexanedione and thus direct conversion to the same products in up to 78% combined yield. The effects of co-solvents, acid co-catalysts and temperature on catalyst activity, decomposition and stability are explored.

1. Introduction and motivation

The hydrodeoxygenation of carbohydrate biomass, *i.e.*, sugars and sugar-derived substrates to value-added chemicals can in principle be realized through an iterative reaction cascade composed of Brønstedt or Lewis acid catalyzed dehydrations of the hydroxyl functions abundant in these substrates and metal catalyzed hydrogenations of the resulting C=C and C=O unsaturation, with the net overall reaction being the removal of oxygen. In principle, both hetero- and homogeneous catalysts can be employed, but beginning with the seminal work by Schiavo et al. [1], heterogeneous systems have to date dominated the research and development endeavour [2–9]. Far fewer examples of homogeneous catalysts for the hydrodexoygenation of polar and water-soluble substrates under acidic conditions have been reported focusing mainly on glycerol and levulinic acid [10–15], with the latter mainly being targeted in ionic liquids or organic solvent medium. Since water is a necessary by-product of the acid catalyzed dehydration steps and the reactions therefore will operate in aqueous medium, such catalysts must – by definition – be water- and acid-stable complexes [16]. In addition, the dehydration of polyalcohol substrates in aqueous conditions empirically requires temperatures in excess of 150 °C. Over the last decade we have engaged in an iterative process of rationally designing, synthesizing, characterizing and testing such catalysts. Scheme 1 shows the structural evolution of the catalyst generations investigated previously (complexes **1**–**4**) [17–22] and the more recent attempts presented and discussed here (complexes **5**–**10**).

* Corresponding author. Fax: +1 519 766 1499.
E-mail address: mschlaf@uoguelph.ca (M. Schlaf).

http://dx.doi.org/10.1016/j.molcata.2015.08.026
1381-1169/

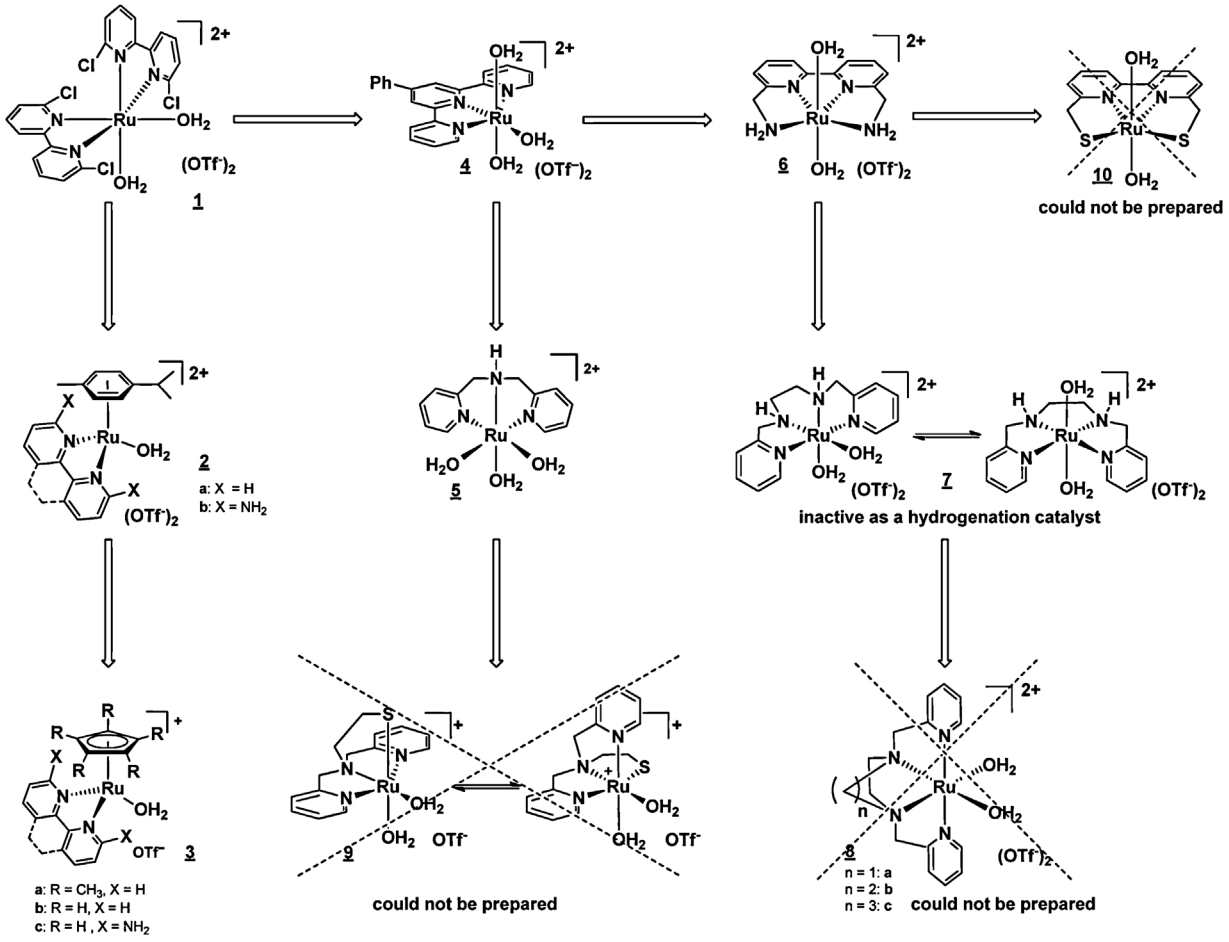

Scheme 1. Structural evolution of water-soluble hydrogenation catalyst investigated and tested.

Acknowledging that an *a priori* and purely theoretically deduced design of catalyst structures and resulting catalytic activity is not possible with present knowledge and therefore has to be based on aspects of both empiricism (*i.e.*, previous knowledge and discovery) and intuition, we targeted the systems shown in Scheme 1 based on the following principles:

1) It is logical to postulate that aquo ligand bearing complexes that can either be isolated or formed *in situ* will be water-stable and – in particular if cationic in nature – also be soluble in water or mixtures of water with other polar solvents.
2) The cationic nature of the metal complexes along with the lability of the aquo ligands, whose metal-ligand binding energy has been estimated to be comparable to a (transient) non-classical dihydrogen ligand [23–25], predisposes these systems to act as ionic hydrogenation catalysts [26], in which dihydrogen gas is heterolytically activated into a hydride ligand on the metal centre without inducing a change in the metal's formal oxidation state and a proton taken up by the counter-ion, solvent, substrate or a proton-shuttle incorporated into the ligand frame-work (*vide infra*). This charge separation process is facilitated by the polar, aqueous reaction medium.
3) Based on both entropy and enthalpy effects [27,28], the use of bi-, tri- and ultimately tetra-dentate chelating ligands should result in increased complex formation constants and hence higher temperature stability. In contrast to typical homogeneous hydrogenation catalysts that operate at low temperature and aim to introduce functionality to the substrate while achieving maximal chemo-, regio- or even enantio-selectivity of the reaction catalyzed, in the hydrodeoxygenation reactions targeted here the goal is to remove functionality from the substrate. The main role of the ligand in these systems is then to prevent reduction and precipitation of bulk metal in oxidation state zero leading to the formation of a heterogeneous catalyst. Our current choice of pyridine and amine rather than phosphine-based ligands is motivated by their anticipated higher long-term stability against air and acidic aqueous media [29–31].
4) Dihydrogen must – at least at elevated pressure – be able to effectively compete with all other ligands present in the reaction mixture. Therefore only non-coordinating or only weakly coordinating solvents (ideally water), auxiliary ligands (*e.g.*, CH_3CN), counter-ions and acid co-catalysts can be employed. In addition, the anion must be hydrolysis and redox-stable, limiting the choices to sulfonic acids such as triflate and triflic acid (as shown in Scheme 1), the strongest non-oxidizing and hence least coordinating acid known [32], and potentially phosphates and phosphoric acid or sulfates and sulfuric acid with the latter two offering substantial cost advantages. However, regardless of which acid is used, in the – necessarily – aqueous reaction medium solvent levelling of any acid to the pK_a of H_3O^+ (−1.74, aqueous scale) will occur.
5) The incorporation of coordinated or pendant amine or thiolate functions that can act as proton-shuttles within the coordination sphere of the metal may lead to a metal-ligand-bifunctional (MLB) hydrogenation mechanism [33–46], facilitating both the heterolytic activation of dihydrogen and the either step-wise or concerted transfer of a proton and hydride to the unsaturated substrate, potentially resulting in overall higher catalyst activity.

Please cite this article in press as: T.A. Minard, et al., J. Mol. Catal. A: Chem. (2015), http://dx.doi.org/10.1016/j.molcata.2015.08.026

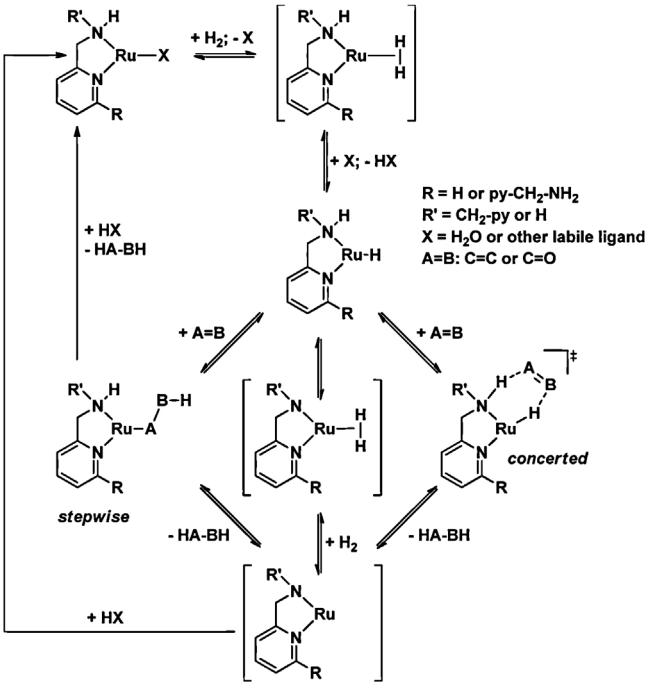

Scheme 2. Conceivable generic catalytic cycle for the hydrogenation of C=C and C=O bonds by catalysts **5**–**7** proposed in Scheme 1 showing possible stepwise and concerted MLB-enhanced reaction pathways and intermediates.

Scheme 2 shows a conceivable generic catalytic cycle using the 2-amino-methylene-pyridine ligand fragment (corresponding to the structural theme of the ligands present in complexes **5**–**7** in Scheme 1) coordinated to ruthenium as an example for possible pathways for the hydrogenation of an unsaturated bond A=B (C=C or C=O). Under the anticipated aqueous acidic conditions, any pendant amines would typically be protonated with the heterolytic activation of dihydrogen occurring through uptake of a proton by the reaction medium, *i.e.*, the counter-ion, substrate, organic co-solvent (if present) or – as stated above – most likely water forming H_3O^+ as the strongest possible acid.

Following some or all of these design principles we previously reported that catalysts **1** and **2** are effective for the hydrodeoxygenation of terminal diols to primary alcohols and – under slightly harsher reaction conditions – alkanes, but decompose by loss of ligand at temperatures >120 °C precluding their use on substrates demanding higher activation temperatures, *i.e.*, glycerol and other sugar alcohols or sugar derivatives and condensates [17,18]. We also established that catalysts **2b** (bipy and phen) do not act as MLB systems, as the pendant amine substitutents of these dicationic systems cannot be protonated by H_3O^+ under aqueous conditions to form the corresponding ammonium substituent, which have an estimated pK_a of <−2. Instead the amine substituted ligands result in catalysts that are less active than the unsubstituted bipy/phen systems **2a**, which was attributed to increased steric hindrance imposed by the presence of the amines.

Recognizing the limitation of these two systems, catalysts **3** and **4** were targeted postulating that replacement of the neutral η^6-arene with an anionic η^5-cp$^{(*)}$ ligand or a tridentate 4′-phenyl-2,2′:6′,2″-terpyridine would enhance the thermal stability and in the case of **3c** – due to the mono-cationic and therefore more electron-rich nature of the complex – allow protonation of the amine substituent by H_3O^+ under solvent-leveled conditions resulting in a MLB enhanced mechanism. A direct comparison of the catalytic activity of **3b** and **3c** in the hydrogenation of ketones did in fact suggest a higher activity for the amine substituted system, which we interpreted as the first example of an MLB enhanced hydrogenation under aqueous acidic conditions [21]. Also in aqueous sulfolane solution both **3** and **4** are stable up 200 °C and effect the partial or total hydrodeoxygenation of glycerol to 1-propanol or propene and propane [20]. Catalyst **4** is also applicable to the hydrodeoxygenation of 2,5-hexanedione and 2,5-dimethyl-furan in water to 2,5-hexanediol, 2,5-dimethyl-THF and hexane in water at temperatures 175–240 °C. However, under these conditions and beginning at 175 °C the catalyst decomposes to the coordinatively saturated and completely inactive bis-chelate $[Ru(4'\text{-Ph-terpy})_2]^{2+}$ and an also inactive Ru^0 coating on the surfaces of the pressure reactor used [22].

The choice of 2,5-hexanedione and 2,5-dimethyl-furan as hydrodeoxygenation substrates stems from them being part of a value-chain leading from glucose to hexane as shown in the previously related Scheme 3 [22,47,48], with the ultimate goal being the identification of promiscuous catalysts systems and reaction parameters that allow a direct conversion of sugars, sugar alcohols and their condensates (*e.g.*, furfural or 5-HMF) to diols, alkenes and alkanes in a single reaction vessel by an iterative hydrodeoxygenation reaction cascade.

As a further logical extension of the series of catalysts **1–4**, we here present the series of complexes **5–7** using the ligands 2,2′-dipicolylamine (dpa), 6,6′-bis(aminomethyl)-2,2′-bipyridine (bambipy) and *N*,*N*′-bis(2-picolyl)ethylenediamine (bpeda). As with **2**, the structures of these potential catalysts were conceived based on the hypotheses that the incorporation of NH or NH_2 functions into the ligand framework would result in a more active MLB-capable (cf. **3c**), but still tri-dentate and hence thermally more stable system (**4** → **5**). Complexes **6**–**8** extend this concept to potentially even more temperature tolerant tetra-dentate systems. Further hypothesizing that the incorporation of thiolate functions would – based on the strong covalent bonds between ruthenium and sulfur (soft/soft interaction) – lead to more electron-rich metal-centres imparting a higher hydricity on any hydride ligand formed and the known ability of thiolate ligands to mediate a heterolytic activation of dihydrogen [49–51], we also considered the pyridine-thiol complexes **9** and **10** as catalyst candidates.

Please cite this article in press as: T.A. Minard, et al., J. Mol. Catal. A: Chem. (2015), http://dx.doi.org/10.1016/j.molcata.2015.08.026

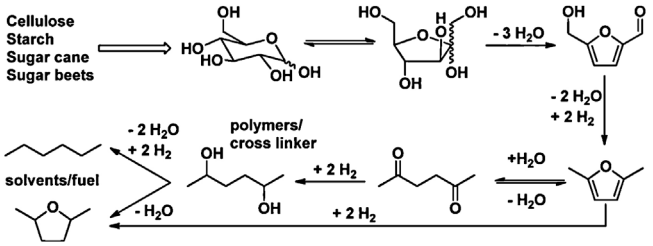

Scheme 3. Value chain leading from glucose to deoxygenated value-added products *via* the two target substrates 2,5-dimethylfuran and 2,5-hexanedione [22].

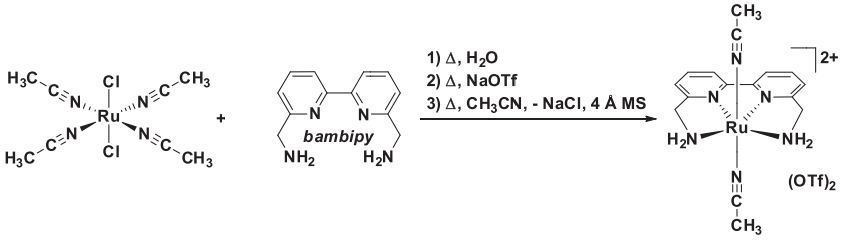

Scheme 4. Synthesis of [*trans*-Ru(CH_3CN)$_2$(bambipy)](OTf)$_2$ (**6a**).

2. Results

2.1. Synthesis of [Ru(2,2′-dipicolylamine)(OH_2)$_3$](OTf)$_2$ (5), [Ru(6,6′-bis(aminomethyl)-2,2′-bipyridine)(OH_2)$_2$](OTf)$_2$ (6) and [Ru(N,N′-bis(2-picolyl)ethylenediamine)(OH_2)$_2$](OTf)$_2$ (7)

Initial attemps to synthesize complexes **5** and **6** followed typical approaches using standard ruthenium chemistry starting materials, *i.e.*, (i) $RuCl_3 \cdot n\ H_2O$ in primary alcohol solvents (combined with subsequent $Ru^{III} \rightarrow Ru^{II}$ reduction by Zn) as successfully employed in the synthesis of catalyst **4** [19,22], (ii) Ru-Blue solutions [52–54], (iii) [*trans*-Ru(CH_3CN)$_4Cl_2$] [55] in various solvents (alcohols, water, CH_3CN, etc.), (iv) [$RuCl_2$(DMSO)$_4$] [56] and (v) [$RuCl_2$(η^6-*p*-cymene)]$_2$ [57] in various solvents where the complexation of dpa or bambipy to ruthenium would be followed by metathesis of the chloride ligands by two equivalents of AgOTf in all cases. None of these attempts yielded defined products in acceptable yields and intractable mixtures of multiple products and/or isomers (by $^1H/^{13}C$ NMR) were obtained regardless of the method employed. A very small amount of deep red crystals could be isolated by diffusion of diethyl ether into a CH_3CN solution obtained from the reaction of [*trans*-Ru(CH_3CN)$_4Cl_2$] with bambipy and NaOTf (Scheme 4) in water. However, the preparation of the CH_3CN solution required the repeated (5–6 times) addition of CH_3CN, filtration of precipitated NaCl and concentration in vacuo (azeotropic distillation) and finally addition of 4 Å molecular sieves to remove water. Single crystal X-ray analysis, ESI–MS, $^1H/^{13}C$ NMR and IR matched the structure shown in Fig. 1 and established the principle ability of the bambipy ligand to coordinate to ruthenium as a tetradentate chelate [58]. While the resulting complex [*trans*-Ru(CH_3CN)$_2$(bambipy)](OTf)$_2$ (**6a**) is in principle usable as a catalyst, this procedure was not practical for the preparation of the material in sufficient quantities for catalysis studies and fails completely for the dpa ligand.

Seeking an alternative method that completely avoids the presence of chloride ligands in the complexation reactions, we decided to adopt the intriguing approach devised by Sardarian et al. who reported the highly efficient *in situ* formation of the tris-chelate complexes [Ru(bipy)$_3$](OTf)$_2$ and [Ru(phen)$_3$](OTf)$_2$ by reaction of excess ligand in *N*,*N*-dimethyl-formamide (DMF) solution with the easily substituted DMF complex [Ru^{II}(DMF)$_6$](OTf)$_2$ [59], which in turn was generated *in situ* by reduction of the corresponding Ru^{III} complex with Platinum black under hydrogen atmosphere as originally described by Judd et al. [60].

In order to avoid the initial *in situ* reduction of $Ru^{III} \rightarrow Ru^{II}$ by Pt/H_2 and replace it with a reduction by Zn or another more easily applied reducing agent after formation of the chelate complexes, we carried out the initial complexation of the dpa and bambipy ligand using [Ru^{III}(DMF)$_6$](OTf)$_3$ in water or aqueous methanol. For both ligands this resulted in a rapid colour change of the solution from pale yellow to deep red over the course of a few minutes and was accompanied by a small amount of gas bubbles forming. To our surprise the ^1H and ^{13}C NMR of the resulting air-stable reaction solutions (generated in D_2O or MeOH-d_4) in both cases showed well defined spectra of a single species with sharp and well resolved resonances distinctly shifted from those of the free ligands indicating that not only complexation, but also *in situ* reduction from the paramagnetic Ru^{III} to a diamagnetic Ru^{II} complexes had occurred. Fig. 2 shows the room temperature evolution of the ^1H NMR spectrum of a D_2O solution of [Ru(DMF)$_6$](OTf)$_3$ and bambipy over 120 min with an observed downfield shift of the ligand resonances, the appearance of free DMF as well as dimethylammonium (DMA). Integration against DMSO as the internal standard also established that no other paramagnetic intermediates whose signals could be broadened into the baseline or lie outside the spectral window recorded are present. A similar spectrum time sequence was recorded for the dpa ligand showing the same effect [61]. Scheme 5 gives the overall reaction for both ligands and product complexes.

The coordination geometry of the bambipy ligand in **6** is assumed to match that of the complex shown in Fig. 1 as it gives very similar ^1H and ^{13}C NMR spectra indicating high symmetry (*trans*-configuration). The actual coordination mode of dpa in complex **5** (*mer vs fac* with only the *fac* isomer shown in Schemes 1 and 5) can due to the symmetry equivalence of the protons in either isomer not be decided by NMR alone and all attempts to grow single crystals suitable for X-ray analysis using multiple solvent/co-solvent combinations failed. However, DFT calculations revealed the *fac* isomer depicted to be ~5.5 kcal/mol more stable. ESI–MS showed peaks with characteristic ruthenium isotope patterns at m/z = 149.50 for the $[Ru(dpa)]^{2+}$ and m/z = 157.88 for $[Ru(bambipy)]^{2+}$ fragments, respectively.

The presence of dimethyl ammonium (identified by separate reference spectra and addition of authentic dimethyl ammonium triflate to the NMR samples) in the reaction solutions suggested a

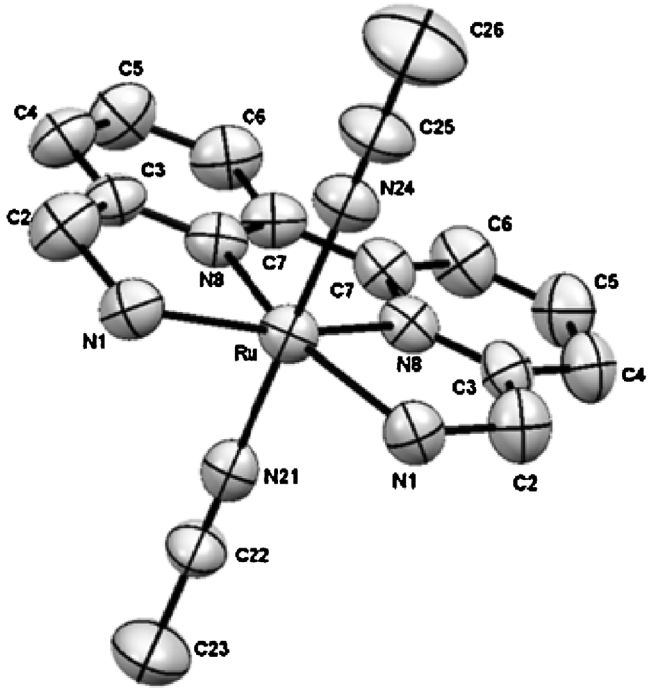

Fig. 1. ORTEP of [*trans*-Ru(CH_3CN)$_2$(bambipy)]$^{2+}$ dication at the 50% probability level. (Hydrogen atoms, disordered triflate counter-ions and CH_3CN solvent molecules present in the unit cell omitted for clarity.)

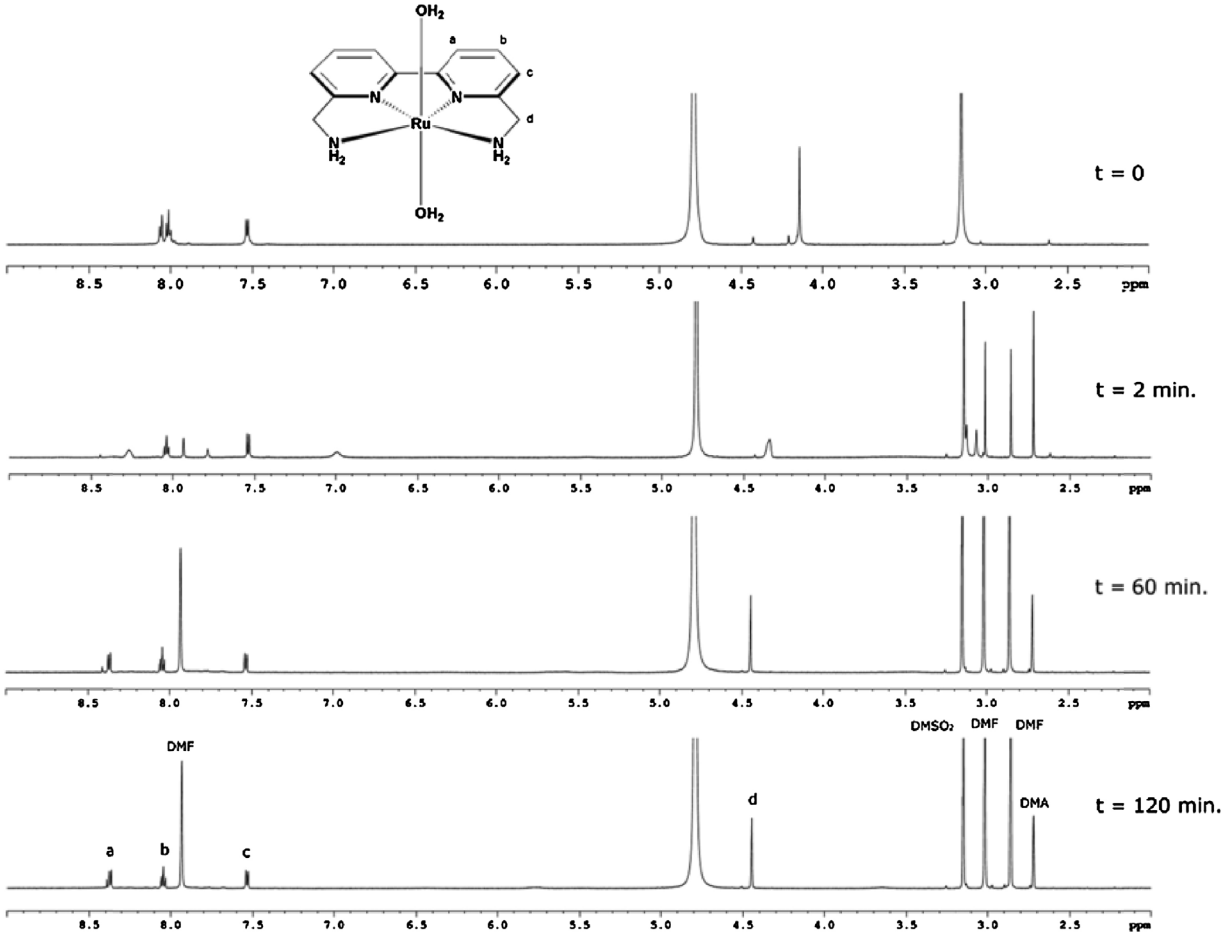

Fig. 2. NMR spectra showing the bambipy ligand (t = 0, top) and the ligand coordinating to Ru at intervals of 2 min, 60 min, and 120 min after addition of [Ru(DMF)$_6$](OTf)$_3$. Note the shifting of the ligand peaks (especially a and d), and appearance of peaks for free DMF and DMA. Recorded at 600 MHz in D_2O, with dimethyl sulfone ($DMSO_2$) used as an internal standard.

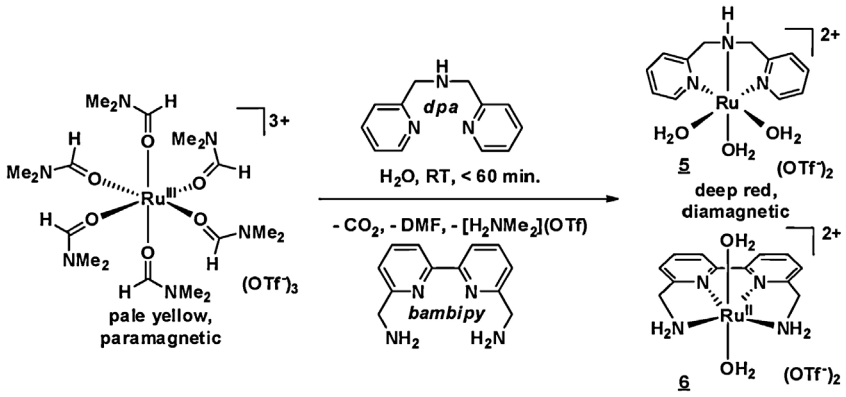

Scheme 5. In situ generation of the dpa and bambipy complexes **5** and **6** by reaction with $[Ru(DMF)_6](OTf)_3$ in water leading to simultaneous complexation and reduction of $Ru^{III} \rightarrow Ru^{II}$.

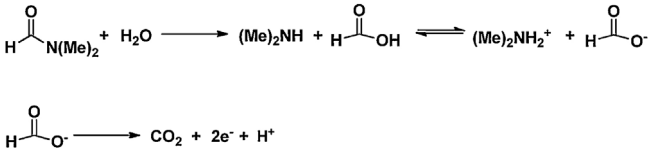

Scheme 6. Decomposition of DMF as the source of reductant for the reactions of Scheme 4.

decomposition of DMF to dimethyl ammonium and ultimately CO_2 (gas evolution—see above) as laid out in Scheme 6 as the source of the reductant for two ruthenium centres ($2\ e^- + 2\ Ru^{III} \rightarrow 2\ Ru^{II}$) in the complexation reactions with a necessary simultaneous formation of an equivalent of free hydronium triflate $[H_3O][OTf]$.

The reaction is analogous to the established use of DMF as a solvent and reducing agent for the formation of silver and gold nano-particles [62], with the added requirement that at ambient temperature the reaction only takes place upon addition of the chelating ligand, *i.e.*, while $[Ru(DMF)_6](OTf)_3$ by itself is stable in water for extended periods of time (in our observations at least hours), the coordination of the ligand to the ruthenium centre either generates free DMF, which can then act as a reducing agent or modifies the electronic environment activating the still coordinated DMF ligand towards nucleophilic attack by water triggering the decomposition reaction of Scheme 6. The bpeda complex [Ru(*N*,*N*′-bis(2-picolyl)ethylenediamine)$(OH_2)_2$](OTf)$_2$ (**7**) can be generated in the same way, but ultimately proved to be only marginally active as a hydrogenation catalyst (*vide infra*).

2.2. Attempted synthesis of complexes 8–10a–c based on the ligands N,N′-bis(2-picolyl) imidazolidine (bipimi), N-N′-bis(2-picolyl) piperazine (bipipi), N,N′-bis(2-picolyl)-homopiperazine (bipipi-h), 2-[bis(2-picolyl)amino]ethanethiol (dpaS) and 2,2′-bipyridine-6,6′-dimethanethiol (dmS_2-bipy)

Hypothesizing that the cause of the inactivity of complex **7** as a catalyst is the additional degrees of freedom afforded by the conformationally flexible ethylenediamine backbone and prompted by the existence of the isoelectronic iron complex *cis*-[Fe(bipipi)(OTf)$_2$] reported by Ostermeier et al. [63], the synthesis of the corresponding ruthenium complexes was attempted. In these complexes the cyclic structure of the 1,*n*-diazocycloalkane ($n = 3$ or 4) ligand backbone would lock the conformation of the ligand, if coordinated in the boat conformation giving the more rigid structures **8a,b,c** as proposed in Scheme 1. However, all attempts using $RuCl_3 \cdot n\ H_2O$, $[Ru(OH_2)_6](OTs)_2$, $[Ru(DMF)_6](OTf)_3$, $[Ru(DMF)_6](OTf)_2$, "Ru-blue", $Ru(acac)_3$, $RuCl_2(DMSO)_4$ or $RuCl_2(NCMe)_4$ either failed to give defined coordination products or resulted in the formation of insoluble resin-like products. Equally all attempts at preparation of the thiolate-ligand complexes [RuL_2(dpaS)](OTf) (**9**) and $RuL_2(dmS_2$-bipy) (**10**) (L = OH_2, CH_3CN, etc.) complexes proved unsuccessful. Again reactions of the ligands with the series of starting materials listed above in various solvents or solvent combinations resulted in decomposition of the ligand and/or ruthenium starting material, generation of a multitude of unidentifiable organic products or production of paramagnetic or what appeared to be insoluble polymeric species. For the dmS_2-bipy ligand in many cases insoluble black precipitates quickly formed upon combination of the ligand with a ruthenium source while in other circumstances the ligand either decomposed or remained in solution unreacted [64].

2.3. Catalytic hydrogenation reactions

Concentrated dark red aqueous solutions (0.5 mL) of **5–7** generated *in situ* by the protocol described above were used directly in catalytic hydrogenation reactions taking into account the small amount of water added by these solutions as detailed in the Experimental Section. The concentrations of the reaction solutions were 1000 mmol/L of substrate and 100 mmol/L dimethylsulfone ($DMSO_2$) as the internal GC standard in all cases. The presence of the inert internal standard allows quantification of the intermediates and products in the complex reaction cascade that evolves from the two substrates investigated in this study with 2,5-hexanedione being two and 2,5-dimethylfuran one step(s) removed from the directly biomass derived 5-hydroxy-methylfurfural as shown in the value-chain in Scheme 3. Importantly, the internal standard also allows the determination of any mass balance deficiencies (MBD) caused by substrate or product oligo- or polymerization to non-volatile products (humins) that cannot be analyzed by GC. Scheme 7 summarizes the overall reaction cascade as also detailed in our previous study using catalyst **4** [22].

Table 1 lists the results of the evaluation of complex **5** for the hydrodeoxygenation of the water-soluble 2,5-hexanedione as a function of temperature and type of acid co-catalyst added. Entries 1-5 show that the complex becomes active as a catalyst at T = 125 °C, reaches an optimum at T = 150 °C and declines in activity at T ≥ 175 °C with catalyst decomposition as indicated by decolouration of the recovered reaction solution from deep red to colourless and the deposition of a shiny pale blue coating on the pressure reactor body. On the basis of control experiments in which fresh substrate solution but no catalyst was added to the reactor this coating is only marginally catalytically active (Entries 15 and 16, Table 1), as also observed in the thermal decomposition of complex **4** [22], while

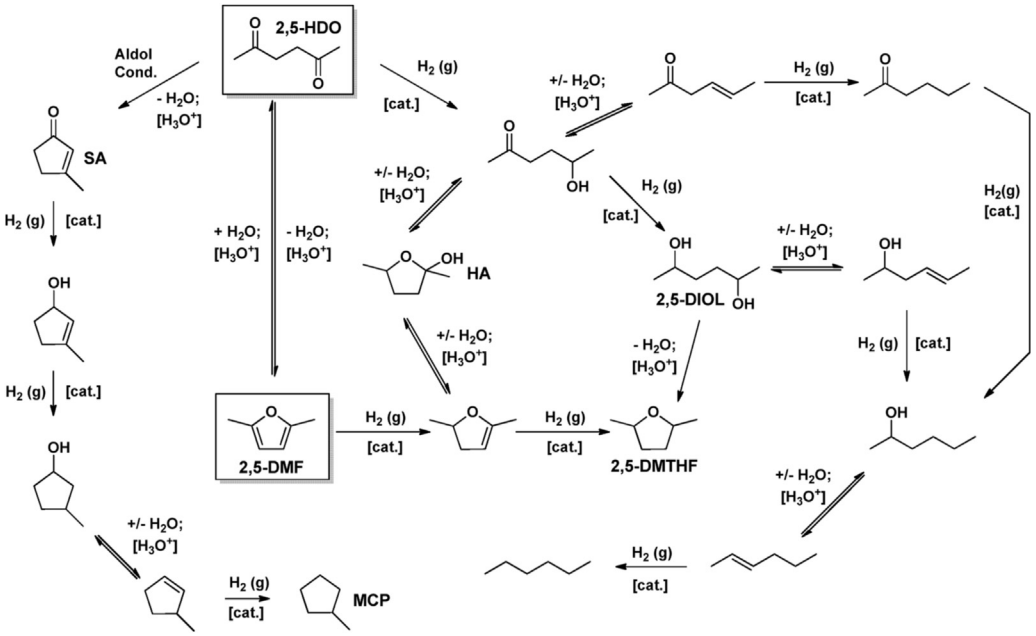

Scheme 7. Reaction cascade for the hydrodeoxygenation of 2,5-hexanedione and 2,5-dimethylfuran under aqueous acidic conditions. (2,5-HDO: 2,5-hexanedione, HA: 2-hydroxy-2,5-dimethyl-tetrahydrofuran ("hemi-acetal"), 2,5-DIOL: 2,5-hexanediol, DMTHF: 2,5-dimethyl-tetrahydrofuran, SA: self-aldol product 3-methyl-cyclopent-2-enone, MCP: methyl-cyclopentane)

Table 1
Hydrodeoxygenation of 2,5-hexanedione by catalyst **5** in water as a function temperature and added co-catalyst.[a]

Entry	T[°C]	Acid/[equiv.][b]	2,5-HDO[%]	HA[%]	2,5-DIOL[%]	DMTHF[%]	SA[%]	MCP[%]	MBD	Catalyst decomp.
1	100	n/a	93	4	0	0	0	0	3	N
2	125	n/a	11	17	37	3	2	0	30	N
3	150	n/a	0	0	94	6	0	0	0	N
4	175	n/a	26	20	18	2	<1	0	34	Y
5	200	n/a	32	20	12	2	0	0	34	Y
6	100	HOTf/10	84	3	1	0	0	0	12	N
7	125	HOTf/10	76	4	2	1	1	0	16	N
8	150	HOTf/10	56	6	3	3	0	0	32	N
9	175	HOTf/10	26	11	6	9	2	0	46	N
10	150	$B(OH)_3$/100	8	9	38	2	6	0	37	Y[c]
11	150	H_3PO_4/100	0	0	0	55	0	2	43	N[d]
12	150	$La(OTf)_3$/100	0	0	88	5	0	0	7	N
13[e]	175	n/a	85	3	1	0	«1	0	11	n/a
14[e]	175	HOTf/10	92	<1	0	<1	«1	0	8	n/a
15[f]	200	n/a	45	12	0	3	0	0	40	n/a
16[f]	200	HOTf/10	74	4	0	0	2	0	20	n/a
17[g]	100	n/a	85	0	0	«1	1	0	14	N
18[g]	150	n/a	2	8	74	3	0	0	13	Y
19[g]	200	n/a	52	13	7	2	0	0	26	Y
20[g]	100	HOTf/10	75	3	0	0	«1	0	22	N
21[g]	150	HOTf/10	10	10	36	1	3	0	40	Y
22[g]	200	HOTf/10	21	1	0	37	0	0	41	Y

2,5-HDO: 2,5-hexanedione, HA: 2-hydroxy-2,5-dimethyl-tetrahydrofuran ("hemi-acetal"), 2,5-DIOL: 2,5-hexanediol, DMTHF: 2,5-dimethyl-tetrahydrofuran, SA: self-aldol product 3-methyl-cyclopentanol, MCP: methyl-cyclopentane), MBD: mass balance deficiency.

[a] Reaction conditions: 2,5-hexanedione [1000 mmol/L], $DMSO_2$ (ISTD) [100 mmol/L], **[**$Ru(2,2'\text{-dipicolylamine})(OH_2)_3](OTf)_2$ (**5**) [1 mmol/L = 0.1 mol% w.r.t to substrate], 5.5 MPa H_2(g) pressure, time = 16 h (overnight), yields by quant, GC.

[b] Equivalents w.r.t. catalyst load.

[c] Catalyst captured in polymerized material.

[d] Phase separation into aqueous and organic phase observed.

[e] Control reaction without added catalyst.

[f] Control reaction with blue coating deposited in reactor body.

[g] $[Ru(DMF)_6](OTf)_3$ without dpa ligand used as the catalyst.

the cleaned reactor body itself is also essentially inactive (Entries 13 and 14, Table 1; see also below and in Section 5).

The effect of temperature on catalyst activity mirrors its stability as observed in an independent NMR experiment. The ^1H spectrum of **5** in D_2O showed no change in appearance upon heating the solution to $T = 125\,^\circ C$, while the presence of several species was detected at $T = 150\,^\circ C$ and decolouration and formation of a black ppt of Ru(0) was observed at $T \geq 175\,^\circ C$. Together these observations support the presence of a homogeneous species as the active species at $T \leq 150\,^\circ C$. Repeating the NMR experiment in the presence of 10 equivalents of HOTf (w.r.t. to Ru) enhanced the stability of the catalyst to $T \geq 175\,^\circ C$. Aiming to push the reaction cascades further towards more or completely deoxygenated products (*i.e.*, ultimately hexane; Scheme 6) this prompted us to explore its activ-

Table 2
Relative activity of catalysts **4** and **5** in the hydrodeoxygenation of 2,5-hexanedione in water with and without added acid co-catalyst (H_3PO_4).[a]

Entry	Catalyst used	Acid/[equiv.][b]	2,5-HDO[%]	HA[%]	2,5-DIOL[%]	DMTHF[%]	SA[%]	MBD
1	4	n/a	29	16	37	11	0	7
2	5	n/a	0	0	94	6	0	0
3	4	H_3PO_4/100	46	0	0	3	<1	51
4	5	H_3PO_4/100	0	0	0	55	2	43

[a] Reaction conditions: 2,5-hexanedione [1000 mmol/L], $DMSO_2$ (ISTD) [100 mmol/L], [(4′-Ph-terpy)$Ru(H_2O)_3$](OTf)$_2$ (**4**) or [Ru(2,2′-dipicolylamine)$(OH_2)_3$](OTf)$_2$ (**5**) [1 mmol/L = 0.1 mol% w.r.t. to substrate], T = 150 °C, 5.5 MPa H_2(g) pressure, time = 16 h (overnight), yields by quant, GC.
[b] Equivalents w.r.t. catalyst load.

Table 3
Hydrodeoxygenation of 2,5-dimethylfuran by catalyst **6** as a function temperature, solvent and added co-catalyst.[a]

Entry	T[°C]	Acid/[equiv.][b]	Solvent	2,5-DMF[%]	2,5-HDO[%]	HA[%]	2,5-DIOL[%]	DMTHF[%]	SA[%]	Hex[%]	MBD[%]	Catalyst decomp.
1	175	n/a	H_2O	0	0	«1	55	23	«1	0	22	N
2	200	n/a	H_2O	0	0	«1	49	13	«1	0	38	N
3	225	n/a	H_2O	0	1	«1	33	11	«1	0	55	Y
4	175	n/a	Diox./H_2O	43	2	2	26	9	2	0	18	N
5	200	n/a	Diox./H_2O	36	3	2	30	7	1	0	18	N
6	225	n/a	Diox./H_2O	16	1	2	50	17	0	0	16	Y
7	175	n/a	Sulf./H_2O	4	76	0	0	0	«1	0	20	N
8	200	n/a	Sulf./H_2O	10	66	0	0	0	«1	0	24	N
9	225	n/a	Sulf./H_2O	16	57	2	<1	<1	«1	0	24	Y
10	175	HOTf/5	Diox./H_2O	4	41	3	3	8	12	0	29	N
11	200	HOTf/5	Diox./H_2O	4	29	0	1	14	10	0	42	N
12	225	HOTf/5	Diox./H_2O	2	14	1	0	17	5	4	56	Y
14[c]	225	n/a	H_2O	2	70	3	3	4	«1	0	17	n/a
15[c]	225	n/a	Diox./H_2O	94	5	0	0	0	«1	0	1	n/a
16[c]	225	n/a	Sulf./H_2O	59	21	0	0	0	0	0	20	n/a

[a] Reaction conditions: 2,5-dimethylfuran [1000 mmol/L], $DMSO_2$ (ISTD) [100 mmol/L], [Ru(6,6′-bis(aminomethyl)-2,2′-bipyridine)$(OH_2)_2$](OTf)$_2$ (**6**) [1 mmol/L = 0.1 mol% w.r.t. to substrate], 5.5 MPa H_2(g) pressure, time = 16 h (overnight), yields by quant, GC.
[b] Equivalents w.r.t. catalyst load.
[c] Control reaction without added catalyst.

ity in the presence of HOTf as well as higher amounts of the weaker Brønstedt acids $B(OH)_3$, H_3PO_4 and the water-soluble and tolerant Lewis acid $La(OTf)_3$ [65]. While the addition of HOTf does in fact stabilize the catalyst it also severely inhibits its activity, achieving a maximum of only 26% of hydrogenated and hydrodeoxygenated products (2,5-DIOL, DMTHF and HA) at 175 °C (Entry 9, Table 1) compared to quantitative conversion at 150 °C without acid. At this optimum reaction temperature the addition of boric acid leads to the formation of an intractable brown solid that also captures the catalyst from the reaction solution as indicated by its decolouration. The addition of H_3PO_4 switches the selectivity to the dehydration ring-closure product 2,5-dimethyl-tetrahydrofuran (DMTHF), but also increases the extent of substrate decomposition likely *via* aldol condensation pathways to non-volatile oligomers that were present as a brown resin in the reactor after reactions. As a trend the addition of Brønstedt acids leads to a higher mass balance deficiency due polymerization of the substrate *via* acid catalyzed aldol-condensation, while he addition of the lanthanide Lewis acid has only a small effect.

On the basis of their structural similarity we also compared the catalytic activity of the tridentate chelate complexes **4** and **5** under identical conditions using the optimum conditions (T = 150 °C) established for the less temperature-stable complex **5** at which the dpa system shows a substantial higher activity both in the presence and absence of H_3PO_4 as the acid co-catalyst. However, we previously found that the 4′-Ph-terpyridine system does not reach its optimum activity until a minimum of T = 175 °C [22].

Attempts to use complex **5** as a catalyst for the hydrodeoxygenation of furfural under the same reaction conditions (no acid added) failed resulting in the formation of a hard organic resin in the reactor with no GC-detectable soluble organic products.

Compared to the tri-dentate dpa complex **5** the tetra-dentate bambipy complex **6** shows only marginal activity for the conversion of 2,5-hexanedione at 150 °C, but achieves high combined yields (>95%) of 2,5-hexanediol and 2,5-dimethyltetrahydrofuran at 175 and 200 °C. Catalyst decomposition and lower activity – again accompanied by deposition of a shiny pale blue coating – is only observed at $T \geq 225$ °C. The higher temperature stability of **6** *vs* **5** allows its use as a catalyst for the hydrodeoxygenation of 2,5-dimethyl-furan, which requires $T \geq 175$ °C for the effective hydrolysis ring-opening to 2,5-hexanedione (Scheme 7) as the actual hydrogenation substrates under aqueous acidic conditions [22,66,67]. As 2,5-dimethylfuran can be obtained from HMF [68–72], this moves the overall reaction cascade closer to actual biomass-derived substrates. Table 3 lists the results of the reactions of 2,5-dimethylfuran with **6** as the catalyst as a function of temperature, solvent system used and acid co-catalyst added. The substrate is only marginally soluble in water at ambient conditions, but the substantial drop of both the relative permittivity (≡dielectric constant ϵ_0) and surface tension σ [mN/m] of water with rising temperature ($\epsilon_0{}^{20} = 80.36 \rightarrow \epsilon_0{}^{150} = 32.32$ and $\sigma^{20} = 72.74 \rightarrow \sigma^{150} = 48.75$, from 20 to 150 °C, respectively and more so at 175–200 °C [73]) increases the solubility of the substrate at higher temperature resulting in homogeneous reaction mixtures.

As oligo- and polymerization side-reactions of the furan do occur in the phase separated situation during the heating up of the reaction mixture [22], we also explored blends of 1,4-dioxane with water (5:1; azeotrope) and sulfolane with water (9:1) as the reaction medium, both of which fully dissolve the substrate and catalyst at room temperature. Regardless of the solvent system used for all reactions with 2,5-dimethylfuran as the substrate, quantitative GC analysis shows varying degrees of a mass balance deficiency (MBD listed in the second last column of Table 3) caused by oligo- or polymerization reactions of the furan with itself or by aldol condensation of the hydrolysate 2,5-hexanedione (as also observed for the reactions listed in Table 1), to non-volatile products that are not captured by the quantitative GC analysis. In water at 175 °C **6** achieves up to 78% conversion to hydrodeoxy-

genated products directly from 2,5-dimethylfuran, but the reaction suffers from increasing mass balance deficiency with increasing temperature (Entries 1–3, Table 3). Switching the solvent system to 1,4-dioxane/water or sulfolane/water (Entries 4–6 and 7–9, Table 3) somewhat suppresses the oligo- or polymerization reactions, but – as also observed with 2,5-hexanedione as the substrate – the use of an organic co-solvent also substantially (for 1,4-dioxane) or completely (for sulfolane) inhibits the catalyst with only the hydrolysis product 2,5-hexanedione being observed. The fairly high yield of hydrodeoxygenated products observed at 225 °C (Entry 6, Table 3) is accompanied by catalyst decomposition making it unlikely that the active species is homogeneous in this case. Attempts to evaluate the effect of acid addition to an aqueous biphasic mixture of 2,5-dimethylfuran and water resulted in the formation of solid deposits even at ambient temperature and as observed in water for 2,5-hexanedione, the addition of acid to the 1,4-dioxane/water medium (Entries 10–12, Table 3) further inhibited catalyst activity. Under the most extreme conditions attempted (Entry 12), a small amount of the total hydrodeoxygenation product hexane was observed, which due to catalyst decomposition to black Ru(0) particles is however attributed to heterogeneous activity and accompanied by a very high degree of substrate decomposition with 56% mass balance deficiency, *i.e.*, the same as observed at this temperature without added acid. A notable solvent effect is the relative abundance of the self-aldol (SA) product 3-methyl-cyclopentanol that can only form after hydrolysis of 2,5-dimethylfuran to the dione [67]. Even though the dione is highly abundant in sulfolane/water only small amounts of self-aldol product are formed, while it is present in substantial amounts in 1,4-dioxane/water under acidic conditions. As the formation of the hemi-acetal (HA) intermediate is contingent on hydrogenation activity, it is only present in small amounts in all inhibited reactions, while in pure water appears to be rapidly further hydrogenated likely existing only in very small steady-state concentrations.

The use of the bpeda complex **7** as a catalyst for the hydrodeoxygenation of 2,5-hexanediol gave only marginal conversions to hydrodeoxygenated products at $T = 150$, 175 and 200 °C. At 225 °C quantitative conversion is observed, which is however accompanied by decolouration of the deep red solution and appearance of a black precipitate of Ru(0) acting as a heterogeneous catalyst.

2.4. Attempt at catalyst reuse

The reusability of the catalyst derived from complex **6** was tested by adding a fresh batch of 2,5-dimethyl-furan solution in water to the red reaction mixture obtained from an experiment at 175 °C in the absence of added acid, which gave the best result without visible catalyst decomposition (Entry 1, Table 3). However, re-pressurizing and re-heating the resulting clear red solution yielded only marginal additional amounts of 2,5-hexanediol and 2,5-dimethyltetrafuran (<10% in each case).

2.5. Control reactions and activity of $[Ru(DMF)_6](OTf)_3$ as a hydrogenation catalyst

Control reactions on the background activity of the 316SS reactor body [74] (Entries 13 and 14, Table 1 and 14–16, Table 3) at 175 °C and at 200 °C with the blue coating resulting from catalyst decomposition of **5** at $T \geq 175$ °C (Entry 16, Table 1) gave only small amounts, typically <5%, of hydrodeoyxgenated products. The activity of the blue coating reaches a maximum combined yield of 12% of the hemi-acetal requiring one hydrogen equivalent and 3% of the 2,5-dimethyltetrahydrofuran requiring two hydrogen equivalents from 2,5-hexanedione (Entry 15, Table 1), which is however still less than half of the combined yield of hydrodeoyxgenated products realized under the same reaction conditions with added catalyst (Entry 5, Table 1). This means that even with the observed catalyst decomposition at this temperature to the blue coating, some of the activity and product distribution is due to the homogeneous catalyst.

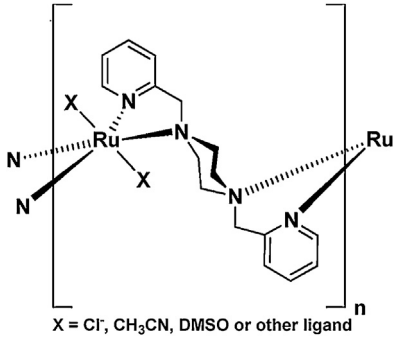

Fig. 3. Coordination of *N*-*N*′-bis(2-picolyl)-1,4-diazocyclohexane in its chair conformation leading to formation of insoluble polymers.

Since the complexes **5** and **6** are generated *in situ*, a further key issue is the actual influence of dpa and bambipy ligand coordination on catalyst activity and stability compared to the $[Ru(DMF)_6](OTf)_3$ precursor itself, *i.e.*, in the absence of a supporting chelate ligand. Entries 17–22 in Table 1 give the results of reactions with 2,5-hexanedione in water in the absence of ligand. At 100 °C essentially no conversion takes place and a clear yellow solution is recovered both with and without added acid. At 150 °C high conversions to 2,5-hexanediol are observed, but are accompanied by decolouration of the solutions and formation of a black precipitate indicating the formation of Ru(0) acting as a heterogeneous catalyst and again a blue coating at the highest temperature of 200 °C at which the overall activity drops and the selectivity switches to 2,5-dimethyltetrahydrofuran in the presence of HOTf. For both **5** and **6** the ligand does therefore play a significant role in activating the metal as a homogeneous catalyst and stabilizing it against reduction to Ru(0).

3. Discussion

3.1. Comments on failed synthesis attempts

As anticipated the tetra-dentate bambipy complex **6** is substantially more temperature-stable than the tri-dentate dpa complex **5** ($T_{max} \geq 175$ *vs* ≤ 150 °C). The availability of other tetra-dentate systems based on the pyridine-chelate motif for testing as catalysts would therefore be highly desirable. As our failed attempts to prepare complexes **8**–**10** show, the synthesis of such complexes is however not trivial, which in our interpretation is due to the following factors:

i) Increasing chelation from tri- to tetradentate ligands places higher demands on the fine-tuning of bond-angles and distances to avoid the introduction of ring-strain that leads to preferential binding *via* bridging rather than chelating modes, as – depending on reaction conditions – observed by Ostermeier et al. for the iron analogue of the proposed complex **8** [63]. The formation of insoluble glassy materials by reaction of various ruthenium precursors with the bipipi and analogous ligands suggests that polymers based on coordination of the diazocycloalkane in the chair conformation are formed (Fig. 3). While higher temperatures should favour the generation of single-metal and hence soluble chelate complexes, predicting which coordination mode is preferred as a function of metal, ligand and reaction conditions applied is not feasible at present requiring the empirical approach described here.

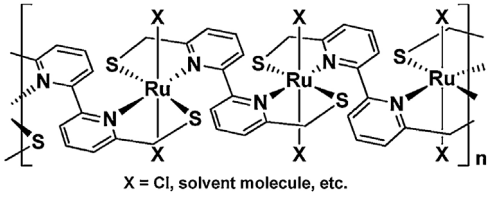

Fig. 4. Possible structure of polymeric species formed by bridging bipy-S_2 ligand.

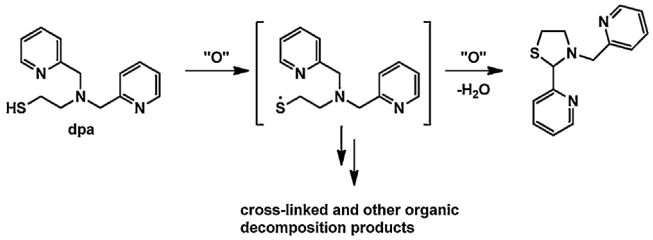

Scheme 8. Oxidation of the dpaSH ligand leading to formation of a thiazolidine ring and/or decomposition.

ii) Comparing the bpeda ligand (used in the only marginally active complex **7**) to the bipimi, bipipi and bipipi-h ligands, the increased steric demand and relatively higher Brønstedt *vs* Lewis basicity (*i.e.*, proton affinity *vs* donor ability) of the tertiary amine are the likely reasons for the failure of these ligands to yield stable coordination products with, *e.g.*, $[Ru(DMF)_6](OTf)_3$, as observed with dpa, bambipy and bpeda all of which contain only primary or secondary amine functions [75].

iii) For the thiolate ligand dmS_2-bipy the failure to yield defined monomeric complexes is – in the cases were coordination is actually observed – again likely routed in the formation of coordination polymers such as shown in Fig. 4, a bridging chelation mode also prevalent with quaterpyridine [76].

For both thiol ligands redox processes, *i.e.*, oxidation of the thiol or thiolate by the metal to radical intermediates and/or disulfides likely also plays a role in the decomposition of the ligand and ligand-metal complexes. This is true even when the less oxidizing Ru^{II} precursors are employed. The oxidation of the dpaSH ligand laid out in Scheme 8 leading to decomposition and cross-linked products is deduced from the presence of small amounts of the thiazolidine in some of the complex reaction mixtures (identified by NMR after chromatographic separation).

3.2. Catalytic reactions

All catalysts investigated require dissociation of an aquo ligand and generation of a free coordination site for the activation of hydrogen. The activation barrier for this process therefore determines the lower temperature limit of their activity, while their upper limit of activity as homogeneous catalysts is defined by loss of the supporting ligand and reduction to Ru(0) or formation of the observed blue coating of unknown composition. In comparison to **4**, **5** is more active for the hydrogenation of 2,5-hexanediol under identical conditions (Table 2), which can however not with any certainty be assigned to an MLB mechanism as proposed in Scheme 2, as **4** only becomes fully active at a temperature that causes **5** to decompose. **5** was therefore not employed for the hydrodeoxygenation of 2,5-dimethylfuran, as its efficient hydrolysis to the actual hydrodeoxygenation substrate 2,5-hexanedione requires $T \geq 150\,^{\circ}C$ [67], but it is highly active for the hydrogenation of 2,5-hexanedione with the product selectivity being switchable from 2,5-hexanediol to the dehydration ring-closure product 2,5-dimethyltetrahydrofuran by the addition of H_3PO_4 as an acid co-catalyst, albeit at a decreased yield for the ring closure product.

Complex **6** displays a very high temperature stability against decomposition to bulk Ru(0), but its effectiveness only marginally improves on that of the previously reported terpyridine based complex **4** [22]. At the catalyst loads investigated (0.1 mol% w.r.t. substrate), neither system is kinetically competent enough to effectively compete with the decomposition of the 2,5-dimethylfuran substrate to non-volatile undefined oligomeric and polymeric products (humins), a process that is even more pronounced for the more reactive furfural or 5-HMF, which were therefore not targeted here.

The heterolytic activation of hydrogen proposed for all catalysts discussed here (Scheme 2) as well as the increasing auto-dissociation of water at elevated temperatures acts as the source of $[H_3O^+]$ as the acid catalyst for the dehydration and ring-opening steps (Scheme 7) [77]. In principle, the addition of more acid should push the dehydration equilibria towards more deoxygenated products and ultimately hexane or possibly methylcyclopentane [78], however both **5** and **6** are inhibited by additional

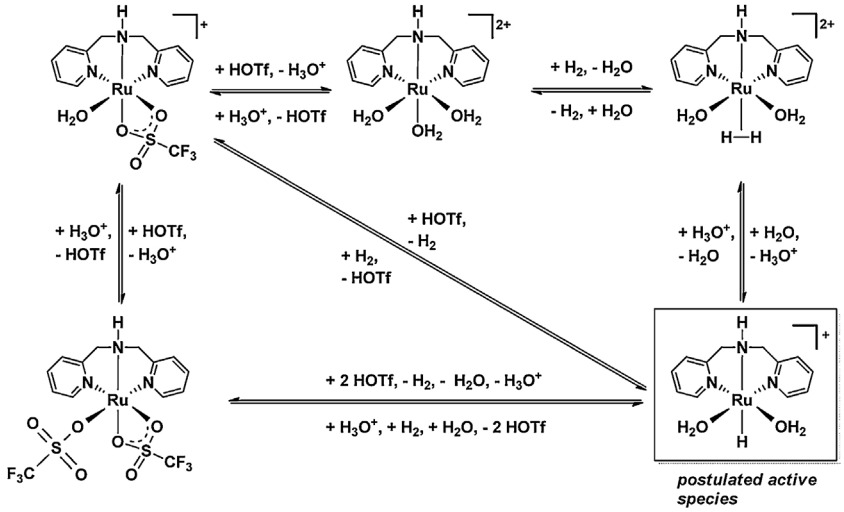

Scheme 9. Conceivable pathways for catalyst inhibition by excess acid using the *fac*-isomer of **5** as an example.

acid, which also increases humin formation as a comparison of Entries 4–6 and 10–12 in Table 3. Causes of the catalyst inhibition could be (i) coordination of the necessarily also introduced counter ion, (ii) inhibition of the heterolytic activation of hydrogen by pushing the H_2 activation equilibrium to the wrong side, *i.e.*, away from the hydride complex as the postulated active species shown on the bottom right in Scheme 9, or (iii) partial dissociation and protonation of the ligand, which would also open an obvious reaction channel for decomposition of the complex, but contradicts the observation that the temperature stability of **5** is enhanced in the presence of excess acid (cf. NMR experiment described above), an effect that may also be related to coordination of the triflate counterion. The inhibition of catalytic activity by addition of sulfonic acids was also observed for **4** [22] and in the catalytic hydrogenation of amides by the Ru(triphos)/methanesulfonic acid system for which Coetzee et al. were able to directly observed coordination of methanesulfonate by NMR [79]. At present the different behavior of H_3PO_4 compared to HOTf (cf. Entry 8 *vs* 11, Table 1) is not well understood, but obviously this acid does specifically facilitate diol dehydration to 2,5-dimethyltetrahydrofuran. The fact that even without visually apparent decomposition reaction solutions of **6** show only marginal activity upon addition of more 2,5-dimethylfuran indicates that catalyst deactivation also occurs by other processes, possibly irreversible coordinative inhibition by substrate and/or intermediate dimers formed by Diels–Alder reactions of the furan or aldol condensations of the dione extending the reaction cascades of Scheme 7 to dimers and oligomers [22].

4. Conclusion

The complexes **5** and **6** described are viable catalysts for the hydrogenation and hydrodeoxygenation 2,5-hexanedione and 2,5-dimethylfuran in water realizing yields of up to 94% of 2,5-hexanediol or 55% of 2,5-dimethyltetrahydrofuran (in the presence of acid co-catalyst H_3PO_4) at 150 °C for **5** from 2,5-hexanedione and up to 55% of 2,5-hexanediol plus 23% of 2,5-dimethyltetrahydrofuran at 175 °C for **6** from 2,5-dimethylfuran. In a single phase the catalysts are however limited by their low tolerance to organic co-solvents needed to solubilize and suppress the decomposition of biomass-derived furan substrates and inhibition by strong acid required as a co-catalyst for further *in situ* dehydration of 2,5-hexanediol to the total hydrodeoxygenation products hexene or hexane. In the presence of excess HOTf selected as a non-coordinating acid co-catalyst or in 1,4-dioxane/water or sulfolane/water blends as the reaction medium **6** is not sufficiently active to compete with the reaction channels leading to formation of involatile humins as expressed by high mass balance deficiencies of the reaction mixture analysis by GC. A successful implementation of homogeneous catalyst systems for the value-chain shown in Scheme 3 or for similar sequences for C5, *i.e.*, xylose derived substrates, and ideally starting from the sugars themselves, will require further enhancement of both activity and relative stability of the catalysts against decomposition, which may be achievable by exploring other permutations of the structural ligand themes laid out in Scheme 1 with an emphasis on the realization of other tetradentate chelate complexes. The use of biphasic reaction mixtures in which water-soluble polar substrates (sugars, sugar alcohols) and intermediates and the acid/metal complex catalyst system are concentrated in an aqueous phase, but less polar intermediates, notably furans, and non-polar products are concentrated or continuously extracted into an inert organic phase may also improve overall performance by limiting coordinative catalyst inhibition and substrate decomposition to involatile or insoluble products.

5. Experimental

All reagents and solvents were purchased from readily available commercial sources and used as received unless otherwise specified. Water was HPLC-grade purified using a Millipore filer and deionizing apparatus. Trifluoromethanesulfonic (triflic) acid was stored under argon atmosphere in a Rotaflo Schlenk tube sealed with a Teflon stopcock. The ligands di(picolyl)amine (dpa) [80], 6,6′-bis(aminomethyl)-2,2′-bipyridine (bambipy) [81,82], *N*,*N*′-bis(2-picolyl)-1,2-ethylenediamine (bpeda) [80], *N*,*N*′-bis(2-picolyl)imidazolidine (bipimi) [83], *N*-*N*′-bis(2-picolyl)piperazine (bipipi) [84], *N*,*N*′-bis(2-picolyl)-homopiperazine (bipipi-h) [84,85], 2-[bis(2-picolyl)amino]ethanethiol (dpaS) [86] and 2,2′-bipyridine-6,6′-dimethanethiol (dmS_2-bipy) [87] and ruthenium complexes $[Ru(DMF)_6](OTf)_3$ [60], $[Ru(H_2O)_6](OTos)_2$ [88,89], *trans*-$[RuCl_2(CH_3CN)_4]$ [55] and $RuCl_2(DMSO)_4$ [56] were prepared following published procedures with – where applicable – the modifications given below. The catalyst [(4′-Phterpy)$Ru(H_2O)_3$](OTf)$_2$] was prepared as previously described [19,22]. Images of NMR and ESI–MS spectra, data and further details are given in the Supplementary material. Catalyst syntheses were performed under argon atmosphere using standard Schlenk-line techniques. All NMR spectra were obtained on Bruker Avance 400 MHz or 600 MHz spectrometers and calibrated to the residual solvent signal. GC analyses were performed on a Varian 3800 with FID detectors using a 30 m Rtx-1701 (14% cyanopropylphenyl/86% dimethyl polysiloxane) column or a 30 m Stabilwax-da (acid-deactivated polyethylene glycol) column. Quantification for 2,5-hexane-dione, 2,5-hexane-diol, 2,5-dimethylfuran and 2,5-dimethyltetrahydrofuran was carried out using internal standard calibration against 100 mmol L^{-1} dimethyl sulfone ($DMSO_2$) at three concentration levels (100, 500 and 1000 mmol/L). All response factors showed a linear relation ($r \geq 0.98$) over the relevant concentration ranges. Other minor intermediates and products (cf. Scheme 6) were quantified using the response factors for these substrates/intermediates/products using the concept of effective carbon number [90]. Headspace gas analyses were carried out on a SRI 8610 micro-GC with a TCD detector against authentic gas samples. (1000 ppm of C_1–C_6 alkanes and C_2–C_6 alkenes in helium, Grace Davison Discovery Sciences). For those reactions where phase separation of an organic product layer occurred the organic layer was weighed, diluted with MeOH and analyzed by GC. No partition of the internal standard $DMSO_2$ from the polar phase into these layers was observed. Assuming equal FID responses for all components of the organic layers (2,5-dimethyltetrahydrofuran and hexane) they were quantified by relative peak areas on the basis of their equal carbon numbers (C6) [90]. Normalization to the molecular weights of the components these gives their relative weights in the organic phase, which were added to the overall yield percentages reported. DFT calculations were carried using the Gaussian 09 software suite [91]. All structures were optimized using the M06-L functional, with def2-SVP basis set and associated ECP for Ru and 6-31G(d,p) basis set for all other atoms. An ultrafine integration grid (99 radial shells with 590 angular points per shell) was used. Solvent effects were incorporated using the polarizable continuum model for water. All structures were verified to be local minima by frequency calculations showing 0 imaginary frequencies. Gibbs free energies reported include zero-point energy corrections and thermal corrections for $T = 298.15$ K and $p = 1.0$ atm. Final evaluation of energies was performed using single point energy calculations on the M06-L/def2-SVP,6-31G(d,p) geometries using the M06-L functional, def2-TZVP basis set with associated ECP for Ru and the 6-311G(d,p) basis set for all other atoms. Zero-point and thermal energy corrections were taken from the lower level geometry optimizations.

Please cite this article in press as: T.A. Minard, et al., J. Mol. Catal. A: Chem. (2015), http://dx.doi.org/10.1016/j.molcata.2015.08.026

All hydrogenation experiments employed industrial grade H_2 gas (99.995%) and were carried out in an Autoclave Engineers (AE) mini-reactor with a 50 mL 316 stainless steel (316SS) reactor vessel and impeller. At a total reaction solution volume of 25 mL the reactor has a gas phase headspace of 50 mL (unused reactor body space and enclosed and pressurized magnet-drive stirring assembly). Unless otherwise specified (cf. control experiments), reactor vessel and impeller were polished thoroughly after every run by lathe at 600 rpm with 3 M abrasive pads or sand-blasting, respectively. Regular control reactions without addition of catalyst showed only marginal conversion (<3%) of substrate to hydrogenated products (see also main text) [74].

5.1. 2,2′-Bipyridine-6,6′-dimethanethiol

The procedure reported by Newkome and Kohli [87] was followed with modification. 2,2′-Bipyridine-6,6′-dimethanethiouronium chloride (2.0086 g, 5.0 mmol) was suspended in water (150 mL), cooled to 5 °C and bubbled with Ar for 1 h. While maintaining the same Ar flow, NaOH (1.5750 g, 39 mmol) was added and the mixture stirred at $T < 10$ °C for 10 min. The solution was then allowed to warm to room temperature and stirred under Ar overnight. The resulting pale yellow solution was washed with 2 × 20 mL TBME, the pH adjusted to 7 with conc. HCl and then extracted with 3 × 50 mL DCM. The organic extracts were dried over Na_2SO_4 and evaporated *in vacuo* providing an off-white solid that was sublimed at 95 °C, 30 m Torr to yield the pure product as a foul smelling white powder that was stored under Ar. Yield: 0.5775 g; 47%. ^{1}H NMR: (400 MHz, $CDCl_3$): δ = 8.34 (*d*, *J* = 7.8 Hz, 2H), 7.80 (*t*, *J* = 7.8 Hz, 2H), 7.37 (*d*, *J* = 7.5 Hz, 2H), 3.94 (*d*, *J* = 7.9 Hz, 4H), 2.14 (*t*, *J* = 7.8 Hz, 2H). ^{13}C NMR: (100 MHz, $CDCl_3$): δ = 159.59 (C), 159.58 (C), 138.05 (CH), 122.60 (CH), 119.73 (CH), 31.01 (CH_2).

5.2. [Ru(OH$_2$)$_3$(di(picolyl)amine)](OTf)$_2$ (5)

0.1105 g (0.112 mmol) of $[Ru(DMF)_6](OTf)_3$ was dissolved in 2.0 mL of degassed (Ar sparge) water. 0.0229 g (0.115 mmol) of di(picolyl)amine (dpa) was dissolved separately in 1.0 mL of H_2O. The di(picolyl) amine solution was then added slowly to the $[Ru(DMF)_6](OTf)_3$ solution and the mixture stirred. A colour change from yellow to deep red was observed after 5 min. ^{1}H NMR (300 MHz, D_2O): δ = 4.369 (s, 2H), 7.383 (*dt*, J_1 = 2.4 Hz, J_2 = 6.3 Hz, 1H), 7.416 (*d*, *J* = 7.8 Hz, 1H), 7.826 (*t*, *J* = 6.6 Hz, 1H), 8.488 (*d*, *J* = 4.2 Hz, 1H). ^{13}C NMR (75 MHz, D_2O): δ = 50.74 (CH_2), 124.29 (CH), 124.61 (CH), 138.91 (CH), 149.04 (CH), 150.10 (CH). ESI–MS for $[Ru(dpa)]^{2+}$ fragment m/z = 149.50.

5.3. [Ru(bambipy)(OH$_2$)$_2$](OTf)$_2$ (6)

$[Ru(DMF)_6](OTf)_3$ (0.0245 g, 0.0248 mmol) and 6,6′-bis(aminomethyl)-2,2′-bipyridine (bambipy) (0.0059, 0.0278 mmol) were combined in a Schlenk tube, which was evacuated and backfilled with argon three times. Degassed (Ar sparge) water (2 mL) was added to this Schlenk tube, which was stirred overnight; solution colour changed from yellow to deep red/orange over the course of a few minutes. ^{1}H NMR (600 MHz, D_2O): δ (ppm) = 4.44 (s, 4H), 7.53 (*d*, *J* = 7.74 Hz, 2H), 8.04 (*t*, *J* = 7.86 Hz, 2H), 8.37 (*d*, *J* = 7.86, 2H). ^{13}C NMR (100 MHz, D_2O): δ (ppm) = 42.80 (CH_2), 121.09 (CH), 122.80 (CH), 138.94 (CH), 151.57 (C), 154.78 (C). ESI–MS $[Ru(bambipy)]^{2+}$ fragment (m/z) = 157.88.

5.4. [trans-Ru(CH$_3$CN)$_2$(bambipy)](OTf)$_2$ (6a)

6,6′-bis(aminomethyl)-2,2′-bipyridine (bambipy) (100 mg, 0.47 mmol, 1.1 equiv.) and *trans*-$[RuCl_2(CH_3CN)_4]$ (144 mg, 0.43 mmol, 1.0 equiv.) were refluxed in degassed H_2O (10 mL) under argon overnight forming a clear red–brown solution. Sodium triflate (153 mg, 0.89 mmol, 2.1 equiv.) dissolved in degassed H_2O (2 mL) was added to the solution, and refluxed for an additional 2 h. The solution was concentrated under vacuum (to ~4 mL), dry acetonitrile was added (~10 mL), and the solution was again concentrated to azeotropically remove H_2O. After this was repeated 4 times, activated molecular sieves (dried under vacuum overnight; slowly heated to 215 °C under vacuum) were added and the solution was stirred for 4 h. The solid was filtered over celite on a filter stick, and the resultant solution was red–purple in colour. The product was crystallized by layering dry diethyl ether over the concentrated acetonitrile solution to generate small amount of deep red crystals. ^{1}H NMR (400 MHz, CD_3CN) δ 2.08 (s, 6H), 4.27 (br. s, 4H), 4.56 (*t*, *J* = 6.0 Hz, 4H), 7.63 (dd, *J* = 0.8 Hz, 8.0 Hz, 2H), 7.92 (*t*, *J* = 8.1 Hz, 2H), 8.18 (dd, *J* = 0.8 Hz, 8.0 Hz, 2H) ^{13}C NMR (100 MHz, CD_3CN) δ 4.3, 54.3, 122.4, 122.7, 126.6, 136.0, 159.0, 164.6. ESI–MS $[Ru(bambipy)]^{2+}$ – 2H fragment (m/z) = 314.01.

5.5. Representative procedure for the preparation of a reaction solution for hydrogenation experiments

(Using the example of 2.5-dimethyl furan in a 5:1 azeotropic mixture of 1,4-dioxane: water in the presence of added acid co-catalyst). Immediately before use 2,5-dimethyl furan was passed through a short plug of neutral alumina to remove impurities and stabilizer present, then added to a 25-mL volumetric flask (2.4033 g, 25 mmol); methyl sulfone (0.2353 g, 2.5 mmol) was also added to this flask as the internal GC standard. The aqueous catalyst solution (≤0.5 mL) was then added to the volumetric flask, along with 1,4-dioxane (10 mL, to maintain 5:1 ratio) and 1.0 mL of a 125 mM triflic acid stock solution (0.125 mmol) (and 5 mL dioxane, to maintain 5:1 ratio). The reaction solution was diluted to 25 mL with a 5:1 1,4-dioxane:water mixture stirred and sonicated to ensure homogeneity.

5.6. Representative procedure for hydrogenation experiments using the AE mini-reactor

A 1 mL sample of the reaction solution was taken for initial GC analysis. (Initial GC analysis can only be performed for reactions with the 2,5-hexanedione substrate as 2,5-dimethylfuran is not miscible with water at ambient conditions and therefore the initial reaction mixtures are biphasic in these cases.) The solution was added to the 50-mL reactor body, which was screwed into the reactor head. The reactor was pressurized with H_2 gas to 5.5 MPa (800 psi) and purged three times, and then held at that pressure to ensure there was no leakage. The system was then heated to the desired temperature (125, 150, 175, 200 or 225 °C) and stirred at 800 rpm for 16 h. The reactor was cooled to ambient temperature, a headspace gas sample was taken for micro-GC analysis, and the reactor depressurized. A 1 mL sample of the final reaction solution is taken for GC analysis.

Acknowledgements

The authors thank the Natural Science and Engineering Council (NSERC) Canada and the Bioeconomy Program of the Ontario Ministry for Agriculture, Food and Rural Affairs (OMAFRA) for supporting this research.

Appendix A. Supplementary data

Supplementary data associated with this article can be found, in the online version, at http://dx.doi.org/10.1016/j.plantsci.2004.08.011.

References

[1] V. Schiavo, G. Descotes, J. Mentech, Bull. Soc. Chim. Fr. 128 (1991) 704–711.
[2] G.W. Huber, S. Iborra, A. Corma, Chem. Rev. 106 (2006) 4044–4098.
[3] A. Corma, S. Iborra, A. Velty, Chem. Rev. 107 (2007) 2411–2502.
[4] D.M. Alonso, J.Q. Bond, J.A. Dumesic, Green Chem. 12 (2010) 1493–1513.
[5] D.M. Alonso, S.G. Wettstein, J.A. Dumesic, Chem. Soc. Rev. 41 (2012) 8075–8098.
[6] P. Gallezot, Chem. Soc. Rev. 41 (2012) 1538–1558.
[7] M. Besson, P. Gallezot, C. Pinel, Chem. Rev. 114 (2014) 1827–1870.
[8] M.J. Climent, A. Corma, S. Iborra, Green Chem. 16 (2014) 516–547.
[9] H. Xiong, H.N. Pham, A.K. Datye, Green Chem. 16 (2014) 4627–4643.
[10] Che, T.; Celanese Corporation, 1987, US Patent 4,642,394.
[11] G. Braca, A.M.R. Galletti, G. Sbrana, J. Organomet. Chem. 417 (1991) 41–49.
[12] F.M.A. Geilen, B. Engendahl, A. Harwardt, W. Marquardt, J. Klankermayer, W. Leitner, Angew. Chem. Int. Ed. 49 (2010) 5510–5514.
[13] F.M.A. Geilen, B. Engendahl, M. Hölscher, J.r. Klankermayer, W. Leitner, J. Am. Chem. Soc. 133 (2011) 14349–14358.
[14] A.S. Gowda, S. Parkin, F.T. Ladipo, Appl. Organomet. Chem. 26 (2012) 86–93.
[15] A. Phanopoulos, A.J.P. White, N.J. Long, P.W. Miller, ACS Catal. 5 (2015) 2500–2512.
[16] M. Schlaf, J. Chem. Soc. Dalton Trans. (2006) 4645–4653.
[17] Z. Xie, M. Schlaf, J. Mol. Catal. A: Chem. 229 (2005) 151–158.
[18] R.R. Dykeman, K.L. Luska, M.E. Thibault, M.D. Jones, M. Schlaf, M. Khanfar, N.J. Taylor, J.F. Britten, L. Harrington, J. Mol. Catal. A: Chem. 277 (2007) 233–251.
[19] D. Taher, M.E. Thibault, D.D. Mondo, M. Jennings, M. Schlaf, Chem. Eur. J. (2009) 10132–10143.
[20] M.E. Thibault, D.V. DiMondo, M. Jennings, P.V. Abdelnur, M.N. Eberlin, M. Schlaf, Green Chem. 13 (2011) 357–366.
[21] D. DiMondo, M.E. Thibault, J. Britten, M. Schlaf, Organometallics 32 (2013) 6541–6554.
[22] R.J. Sullivan, E. Latifi, B.K.M. Chung, D.V. Soldatov, M. Schlaf, ACS Catal. (2014) 4116–4128.
[23] G. Kubas, Metal dihydrogen and σ-bond complexes, in: Structure, Theory and Reactivity, Kluwer Academic/Plenum Publishers, New York, 2001.
[24] N. Aebischer, U. Frey, A. Merbach, Chem. Commun. (1998) 2303–2304.
[25] P.V. Grundler, O.V. Yazyev, N. Aebischer, L. Helm, G. Laurenczy, A.E. Merbach, Inorg. Chim. Acta 359 (2006) 1795–1806.
[26] R.M. Bullock, Chem. Eur. J. 10 (2004) 2366–2374.
[27] R.D. Hancock, J. Chem. Educ. 69 (1992) 615–621.
[28] A.E. Martell, R.D. Hancock, R.J. Motekaitis, Coord. Chem. Rev. 133 (1994) 39–65.
[29] C. Larpent, R. Dabard, H. Patin, New J. Chem. 12 (1988) 907–913.
[30] C. Larpent, R. Dabard, H. Patin, Inorg. Chem. 26 (1987) 2922–2924.
[31] C. Larpent, H. Patin, J. Organomet. Chem. 335 (1987) C13–C16.
[32] R.D. Howells, J.D.M. Crown, Chem. Rev. 77 (1977) 69–92.
[33] Y. Blum, Y. Shvo, J. Organomet. Chem. 282 (1985) C7–C10.
[34] Y. Blum, D. Czarkie, Y. Rahamin, Y. Shvo, Organometallics 4 (1985) 1459–1461.
[35] Y. Shvo, D. Czarkie, Y. Rahamin, J. Am. Chem. Soc. 108 (1986) 7400–7402.
[36] S. Hashiguchi, A. Fujii, K.-J. Haack, K. Matsumura, T. Ikariya, R. Noyori, Angew. Chem. Int. Ed. Engl. 36 (1997) 288–290.
[37] K.-J. Haack, S. Hashiguchi, A. Fujii, T. Ikariya, R. Noyori, Angew. Chem. Int. Ed. Engl. 36 (1997) 285–288.
[38] H.S. Chu, C.P. Lau, K.Y. Wong, W.T. Wong, Organometallics 17 (1998) 2768–2777.
[39] D.H. Lee, B.P. Patel, E. Clot, O. Eisenstein, R.H. Crabtree, Chem. Commun. (1999) 297–298.
[40] R. Noyori, M. Yamakawa, S. Hashiguchi, J. Org. Chem. 66 (2001) 7931–7944.
[41] T. Ohkuma, D. Ishii, H. Takeno, R. Noyori, J. Am. Chem. Soc. 122 (2000) 6510–6511.
[42] K. Abdur-Rashid, S.E. Clapham, A. Hadzovic, J.N. Harvey, A.J. Lough, R.H. Morris, JACS 124 (2002) 15104–15118.
[43] S.E. Clapham, A. Hadzovic, R.H. Morris, Coord. Chem. Rev. 248 (2004) 2201–2237.
[44] C.A. Sandoval, T. Ohkuma, N. Utsumi, K. Tsutsumi, K. Murata, R. Noyori, Chem. Asian J. 1 (2006) 102–110.
[45] M. Ito, T. Ikariya, Chem. Commun. (2007) 5134–5142.
[46] W.W.N. O, A.J. Lough, R.H. Morris, Organometallics 31 (2012) 2137–2151.
[47] R. Palkovits, ChemSusChem 8 (2015) 755–757.
[48] B. Saha, M.M. Abu-Omar, ChemSusChem 8 (2015) 1133–1142.
[49] M. Schlaf, R.H. Morris, J. Chem. Soc. Chem. Commun. (1995) 625–626.
[50] M. Schlaf, A.J. Lough, R.H. Morris, Organometallics 15 (1996) 4423–4436.
[51] D. Sellmann, G.H. Rackelmann, F.W. Heinemann, Chem. Eur. J. 3 (1997) 2071–2080.
[52] J.D. Gilbert, D. Rose, G. Wilkinson, J. Chem. Soc. (A) (1970) 2765–2769.
[53] D. Rose, G. Wilkinson, J. Chem. Soc. (A) (1970) 1791–1795.
[54] T. Togano, N. Nagao, M. Tsuchida, H. Kumakura, K. Hisamatsu, F.S. Howell, M. Mukaida, Inorg. Chim. Acta 195 (1992) 221–225.
[55] B.F.G. Johnson, J. Lewis, I.E. Ryder, Dalton Trans. (1977) 719–724.
[56] I.I. Bratsos, E. Alessio, Inorg. Synth. 35 (2010) 148–152.
[57] M.A. Bennett, T.-N. Huang, T.W. Matheson, A.K. Smith, η^6-Hexamethylbenzene)ruthenium complexes, in: J.P. Fackler (Ed.), Inorg. Synth., John Wiley & Sons, New York, 1982, pp. 74–77.
[58] The CIF for this structure as well as further experimental details and images of NMR spectra for all relevant ligands and complexes described are given in compound data sheets contained in the Supplementary material.
[59] A. Sardarian, B.J. Coe, K.T. Douglas, Transit. Met. Chem. 28 (2003) 905–907.
[60] R.J. Judd, R. Cao, M. Biner, T. Armbruster, H.-B. Buergi, A.E. Merbach, A. Ludi, Inorg. Chem. 34 (1995) 5080–5083.
[61] See Supplementary material for an image of these spectra.
[62] I. Pastoriza-Santos, L.M. Liz-Marzan, Adv. Funct. Mater. 19 (2009) 679–688.
[63] M. Ostermeier, C. Limberg, B. Ziemer, Z. Anorg, Allg. Chem. 632 (2006) 1287–1292.
[64] M. Ryan Sullivan, M.Sc. Thesis, University of Guelph, 2015.
[65] S. Kobayashi, Synlett (1994) 689–701.
[66] A.D. Sutton, F.D. Waldie, R. Wu, M. Schlaf, L.A. 'Pete' Silks, J.C. Gordon, Nat. Chem. 5 (2013) 428–432.
[67] B. Kuhlmann, E.M. Arnett, M. Siskin, J. Org. Chem. 59 (1994) 3098–3101.
[68] Y. Roman-Leshkov, C.J. Barrett, Z.Y. Liu, J.A. Dumesic, Nature 447 (2007) 982–985.
[69] J. Jae, W.Q. Zheng, R.F. Lobo, D.G. Vlachos, ChemSusChem 6 (2013) 1158–1162.
[70] Y.B. Huang, M.Y. Chen, L. Yan, Q.X. Guo, Y. Fu, ChemSusChem 7 (2014) 1068–1072.
[71] M. Chidambaram, A.T. Bell, Green Chem. 12 (2010) 1253–1262.
[72] T. Thananatthanachon, T.B. Rauchfuss, Angew. Chem. Int. Ed. 49 (2010) 6616–6618.
[73] See http://www.iapws.org/release.html for the up-to-date collection of physical data on water.
[74] D. Di Mondo, D. Ashok, F. Waldie, N. Schrier, M. Morrison, M. Schlaf, ACS Catal. (2011) 355–364.
[75] Carrying out this reaction at higher pH leads to precipitation of undefined ruthenium hydroxide species.
[76] R. Zong, R.P. Thummel, J. Am. Chem. Soc. 126 (2004) 10800–10801.
[77] At 150–250 °C the pK_w of water drops from 14.00 at 25 °C to 11.64–11.20, i.e., the relative concentration of hydronium H_3O^+ (and hydroxide OH^-) is approximately three orders of magnitude higher than at room temperature.
[78] E.R. Sacia, M.H. Deaner, Y. Louie, A.T. Bell, Green Chem. 17 (2015) 2393–2397.
[79] J. Coetzee, D.L. Dodds, J. Klankermayer, S. Brosinski, W. Leitner, A.M.Z. Slawin, D.J. Cole-Hamilton, Chem. Eur. J. 19 (2013) 11039–11050.
[80] D.W. Gruenwedel, Inorg. Chem. 7 (1968) 495–501.
[81] T.M. Cassol, F.W.J. Demnitz, M. Navarro, E.A.D. Neves, Tetrahedron Lett. 41 (2000) 8203–8206.
[82] Z. Wang, J. Reibenspies, R.J. Motekaitis, A.E. Martell, J. Chem. Soc. Dalton Trans. (1995) 1511–1518.
[83] C. Baffert, M.-N. Collomb, A. Deronzier, S. Kjaergaard-Knudsen, J.-M. Latour, K.H. Lund, C.J. McKenzie, M. Mortensen, L.P. Nielsen, N. Thorup, Dalton Trans. (2003) 1765–1772.
[84] I. Castillo, V. Perez, I. Monsalvo, P. Demare, I. Regla, Inorg. Chem. Commun. 38 (2013) 1–4.
[85] J.A. Halfen, J.M. Uhan, D.C. Fox, M.P. Mehn, L. Que Jr., Inorg. Chem. 39 (2000) 4913–4920.
[86] N. Lazarova, J. Babich, J. Valliant, P. Schaffer, S. James, J. Zubieta, Inorg. Chem. 44 (2005) 6763–6770.
[87] G.R. Newkome, D.K. Kohli, Heterocycles 15 (1981) 739–742.
[88] P. Bernhard, H.B. Buergi, J. Hauser, H. Lehmann, A. Ludi, Inorg. Chem. 21 (1982) 3936–3941.
[89] P. Bernhard, M. Biner, A. Ludi, Polyhedron 9 (1990) 1095–1097.
[90] J.T. Scanlon, D.E. Willis, J. Chromatogr. Sci. 23 (1985) 333–340.
[91] M.J. Frisch, G.W. Trucks, H.B. Schlegel, G.E. Scuseria, M.A. Robb, J.R. Cheeseman, G. Scalmani, V. Barone, B. Mennucci, G.A. Petersson, H. Nakatsuji, M. Caricato, X. Li, H.P. Hratchian, A.F. Izmaylov, J. Bloino, G. Zheng, J.L. Sonnenberg, M. Hada, M. Ehara, K. Toyota, R. Fukuda, J. Hasegawa, M. Ishida, T. Nakajima, Y. Honda, O. Kitao, H. Nakai, T. Vreven, J.A. Montgomery Jr., J.E. Peralta, F. Ogliaro, M.J. Bearpark, J. Heyd, E.N. Brothers, K.N. Kudin, V.N. Staroverov, R. Kobayashi, J. Normand, K. Raghavachari, A.P. Rendell, J.C. Burant, S.S. Iyengar, J. Tomasi, M. Cossi, N. Rega, N.J. Millam, M. Klene, J.E. Knox, J.B. Cross, V. Bakken, C. Adamo, J. Jaramillo, R. Gomperts, R.E. Stratmann, O. Yazyev, A.J. Austin, R. Cammi, C. Pomelli, J.W. Ochterski, R.L. Martin, K. Morokuma, V.G. Zakrzewski, G.A. Voth, P. Salvador, J.J. Dannenberg, S. Dapprich, A.D. Daniels, Ö. Farkas, J.B. Foresman, J.V. Ortiz, J. Cioslowski, D.J. Fox, Gaussian, Inc., Wallingford, CT, USA, (2009).

Please cite this article in press as: T.A. Minard, et al., J. Mol. Catal. A: Chem. (2015), http://dx.doi.org/10.1016/j.molcata.2015.08.026